Open Access
ChemistryOPEN

Supporting Information

Insights into Allosteric Control of Human Blood Group A and B Glycosyltransferases from Dynamic NMR

Friedemann Flügge and Thomas Peters*

Supporting Information

Insights into allosteric control of human blood group A and B glycosyltransferases from dynamic NMR

Friedemann Flügge and Thomas Peters

CONTENTS

Figures

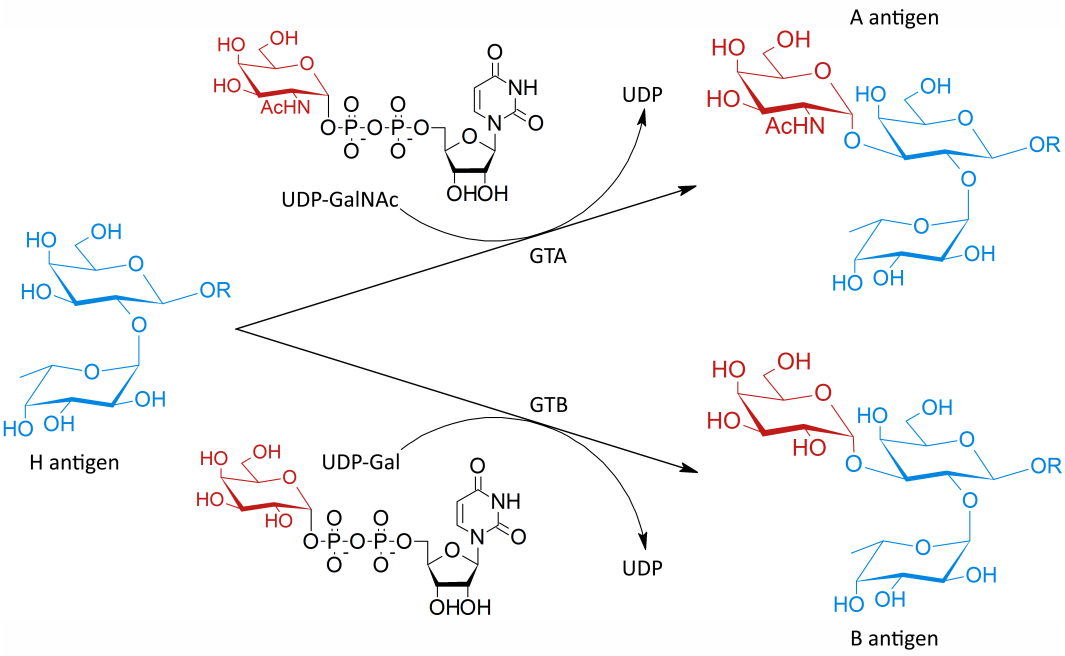

Figure S1 - Glycosyltransfer catalyzed by GTA and GTB. GTA/GTB catalyzed formation of blood group A and B antigens. Catalysis requires the presence of Mn^{2+} ions. For NMR experiments Mg^{2+} is used as a substitute for Mn^{2+} leading to slower catalysis (see main text). For a review on mechanistic aspects of glycosyltransferases see Breton et al. [1].

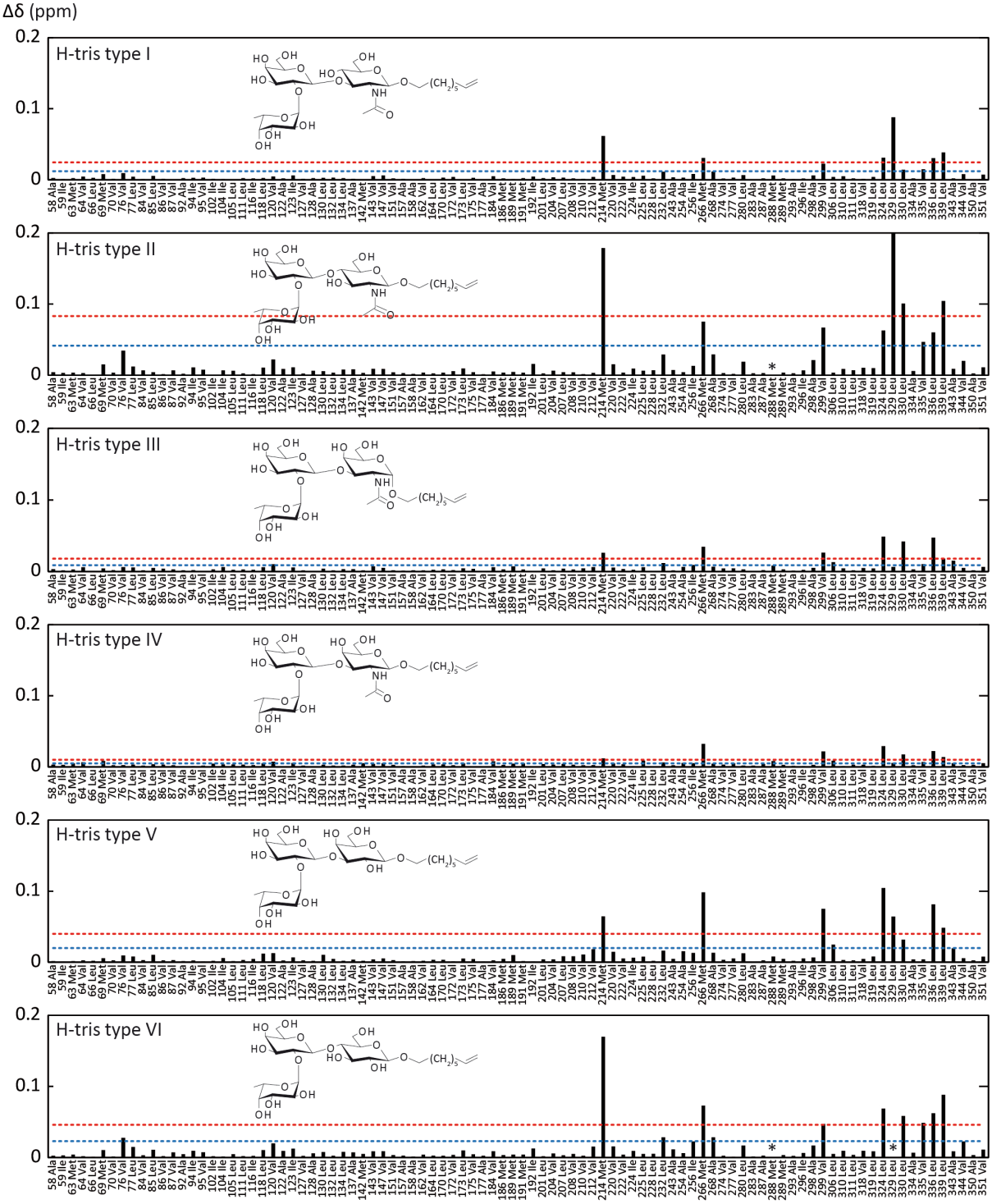

Figure S2 - CSPs for H-trisaccharides (acceptor substrates) binding to GTB. Residue specific CSPs observed for binding of different H-trisaccharide antigens (acceptor substrates, see also Scheme 1 of the main text) to GTB. Shown are the weighted Euclidean distances between peak positions in 2D [^{13}C,^{1}H]-HMQC spectra of apo-GTB and of GTB in presence of H-trisaccharide antigens. Spectra were recorded with AIL^{proS}MV^{proS} GTB (180 µM) and excess of ligand (3120 µM). Residues are listed in sequential order. The dashed lines indicate cut-offs at 1σ (blue) and 2σ (red).

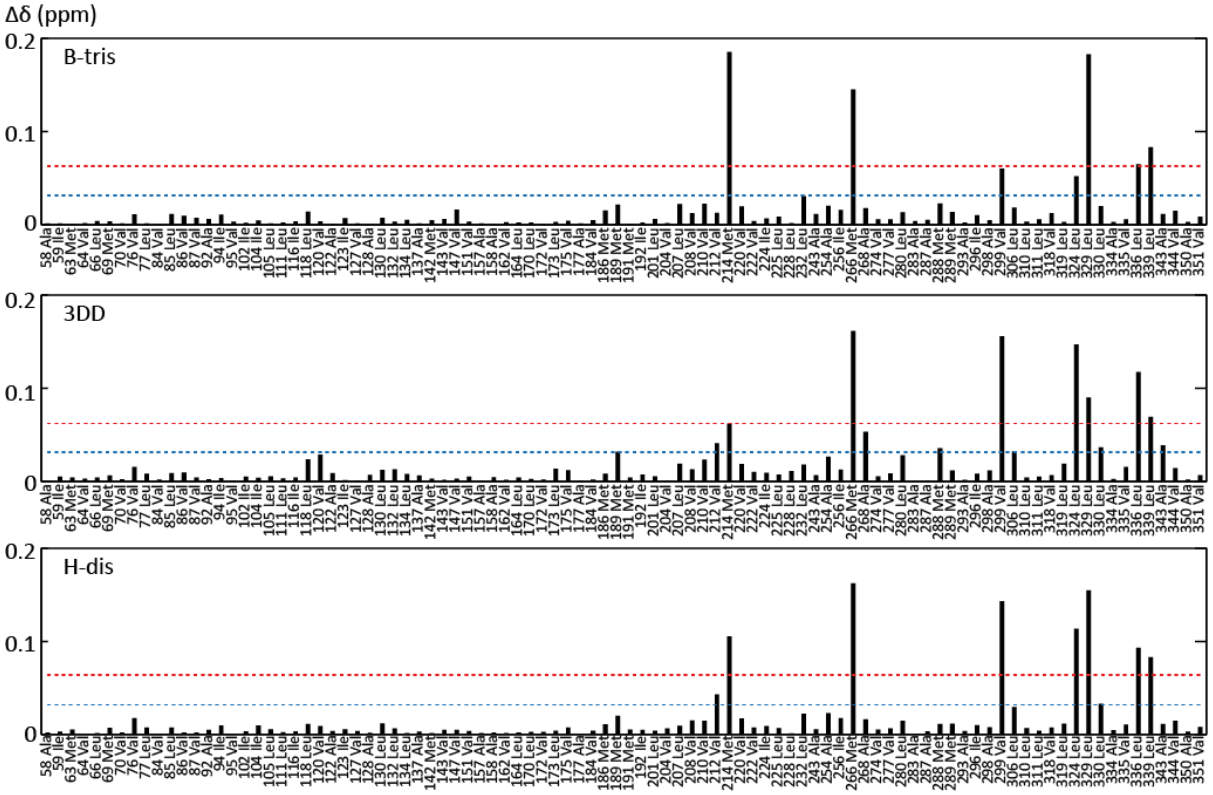

Figure S3 - CSPs for B-Tris, 3DD, and H-Dis binding to GTB. Residue specific CSPs observed for binding of the product of glycosylation, B-trisaccharide, a mock acceptor substrate, 3DD, and the acceptor substrate H-disaccharide to the acceptor binding site of GTB. The three panels show the weighted Euclidean distances between peak positions in 2D [^{13}C,^{1}H]-HMQC spectra of apo-GTB and of ligand-saturated GTB, respectively. Spectra were recorded with AIL^{proS}MV^{proS} GTB (270 µM) and excess of ligand (1120 µM). Residues are listed in sequential order. The dashed lines indicate cutoffs at 1σ (blue) and 2σ (red).

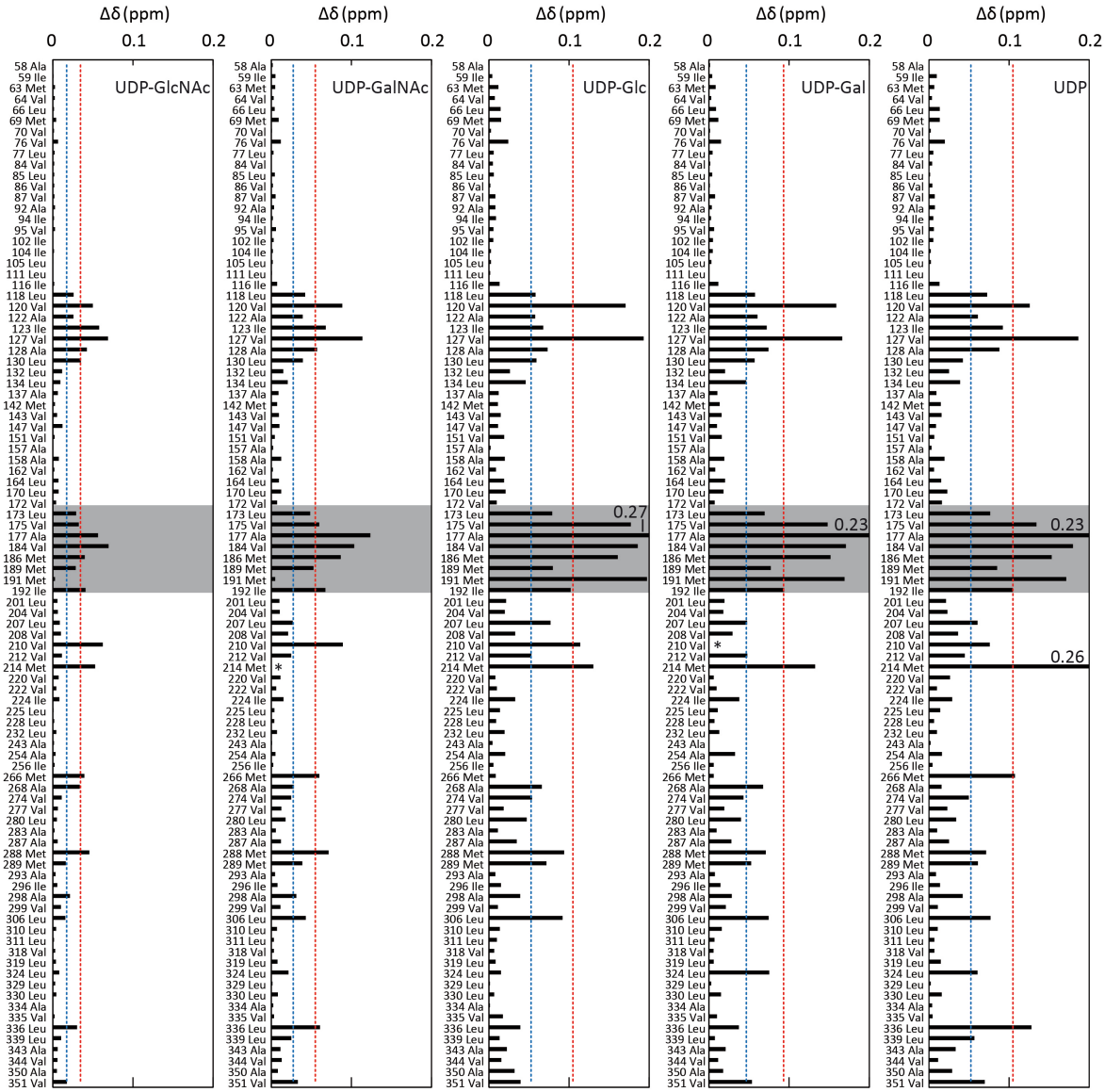

Figure S4 - CSPs for donor-type ligands binding to GTB. Residue specific CSPs observed for binding of donor-type ligands to the donor binding site of GTB. The five panels show the weighted Euclidean distances (Δδ) between peak positions in 2D [^{13}C,^{1}H]-HMQC spectra of apo-GTB and of ligand-saturated GTB. Spectra were recorded with AIL^{proS}MV^{proS} GTB (270 µM) and high excess of ligands (6200 µM). Residues are listed in sequential order. The dashed lines indicate cutoffs at 1σ (blue) and 2σ (red). The internal disordered loop is highlighted in grey. Chemical shift perturbations greater than 0.2 ppm are given at the respective bars. Ambiguous CSPs are labeled with *.

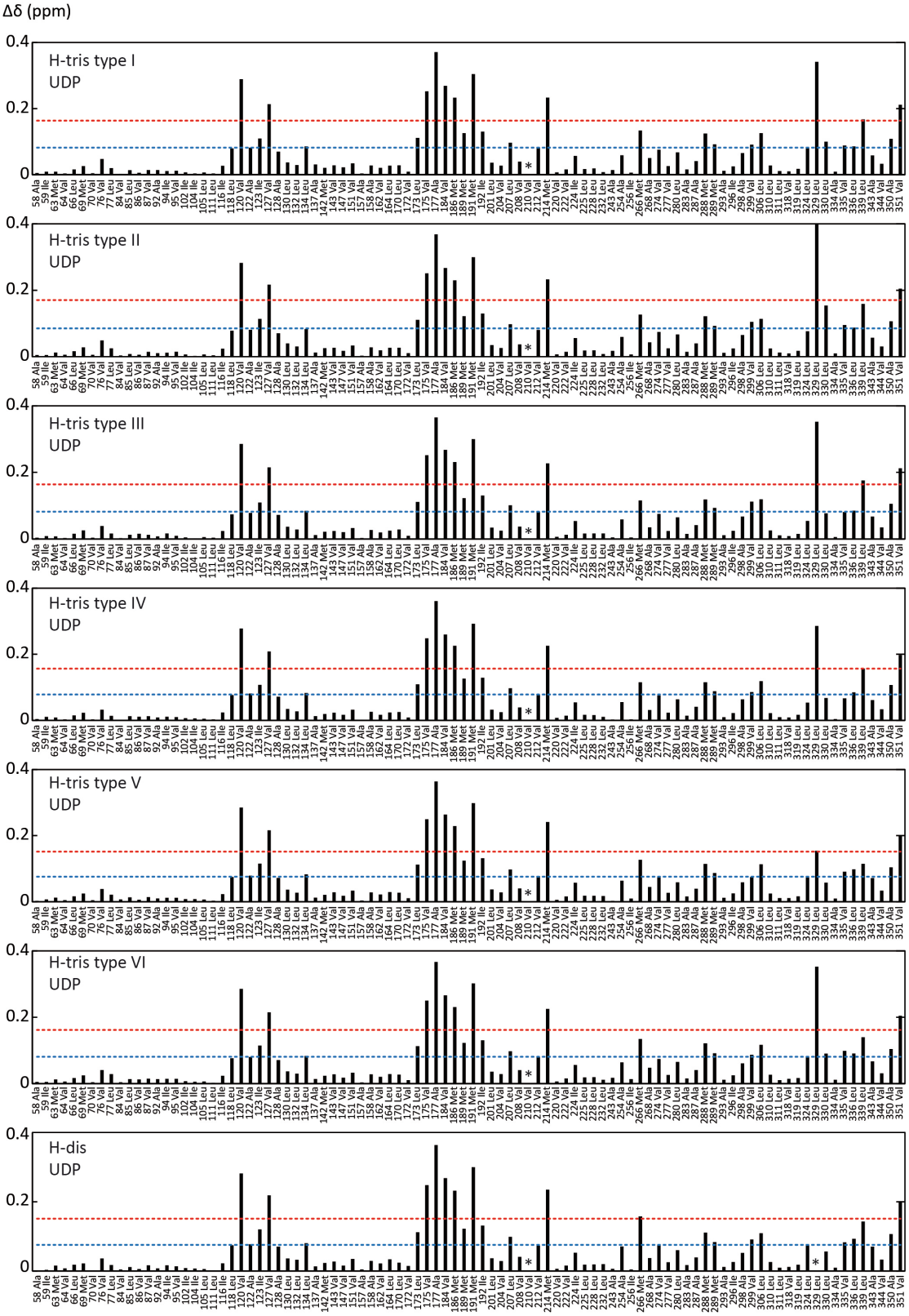

Figure S5 - CSPs for H-trisaccharides (acceptor substrates) binding to GTB:UDP. Residue specific CSPs observed for binding of different H-trisaccharide antigens and H-disaccharide (acceptor substrates) and UDP (donor-type ligand) to GTB. Shown are the weighted Euclidean distances between peak positions in 2D [^{13}C, ^{1}H]-HMQC spectra of apo-GTB, and of GTB in presence of UDP and H-antigens. Spectra were recorded with AIL^{proS}MV^{proS} GTB (180 μM) and excess of UDP (6800 μM) and H-antigens (3120 μM). Residues are listed in sequential order. The dashed lines indicate cut-offs at 1σ (blue) and 2σ (red).

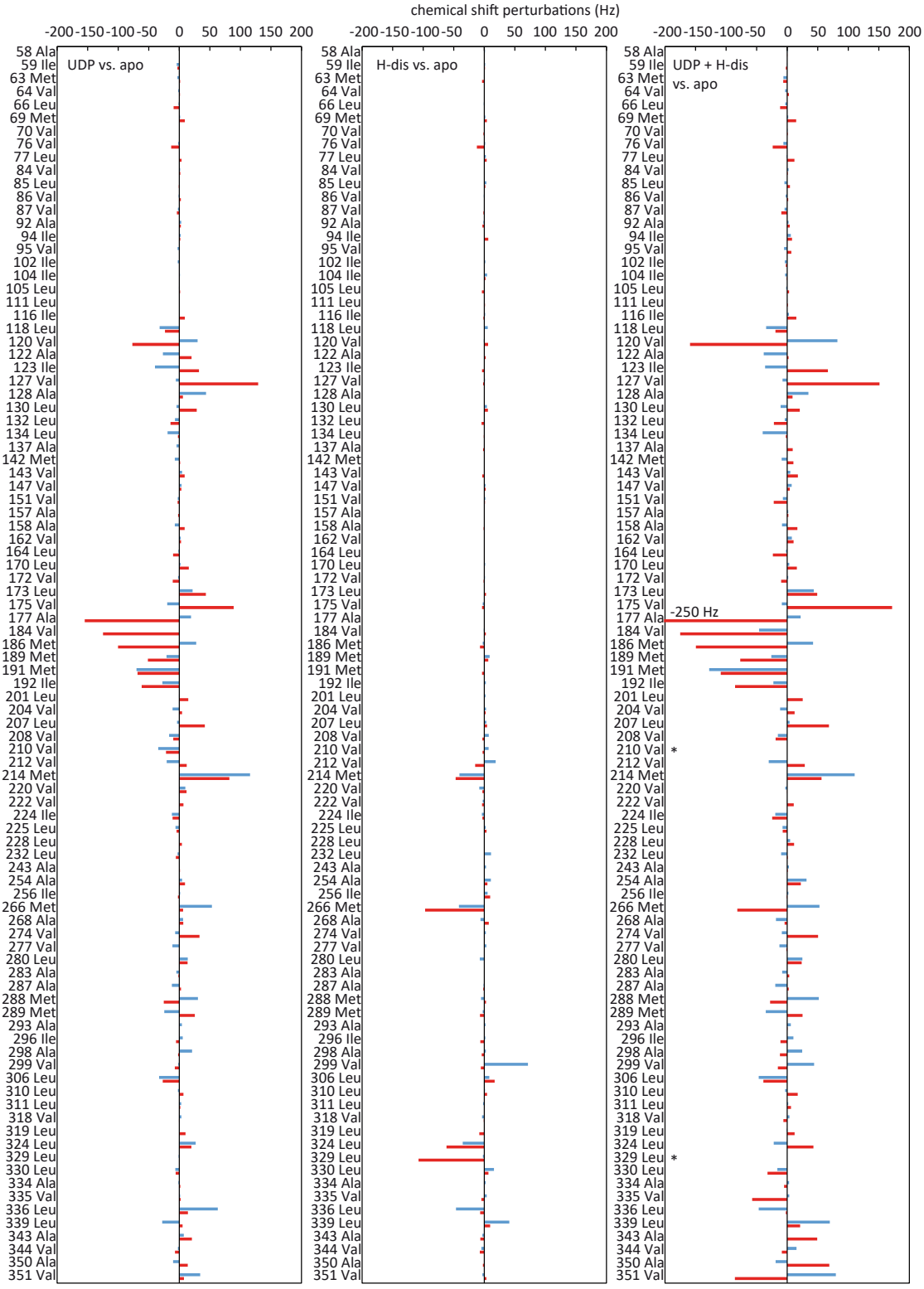

Figure S6 - ^{1}H and ^{13}C CSPs for GTB:UDP, GTB:H-Dis, and GTB:UDP:H-Dis. ^{1}H (red) and ^{13}C (blue) residue specific CSPs for UDP (donor-type ligand) and H-disaccharide (acceptor substrate) binding to GTB. The concentrations were: 280 μM GTB, 6.2 mM UDP, 1.12 mM H-disaccharide (H-Dis). *Left panel:* GTB:UDP. *Middle panel:* GTB:H-Dis. *Right panel:* GTB:UDP:H-Dis. Upon simultaneous binding of UDP and H-Dis CSPs in the internal disordered loop (residues 173-192) are enhanced and not reversed, excluding competition and supporting the presence of allosteric interactions between acceptor and donor binding. The CSPs observed in the right panel for the C-terminal amino acids of GTB reflect ordering of the C-terminus upon binding of both ligands.

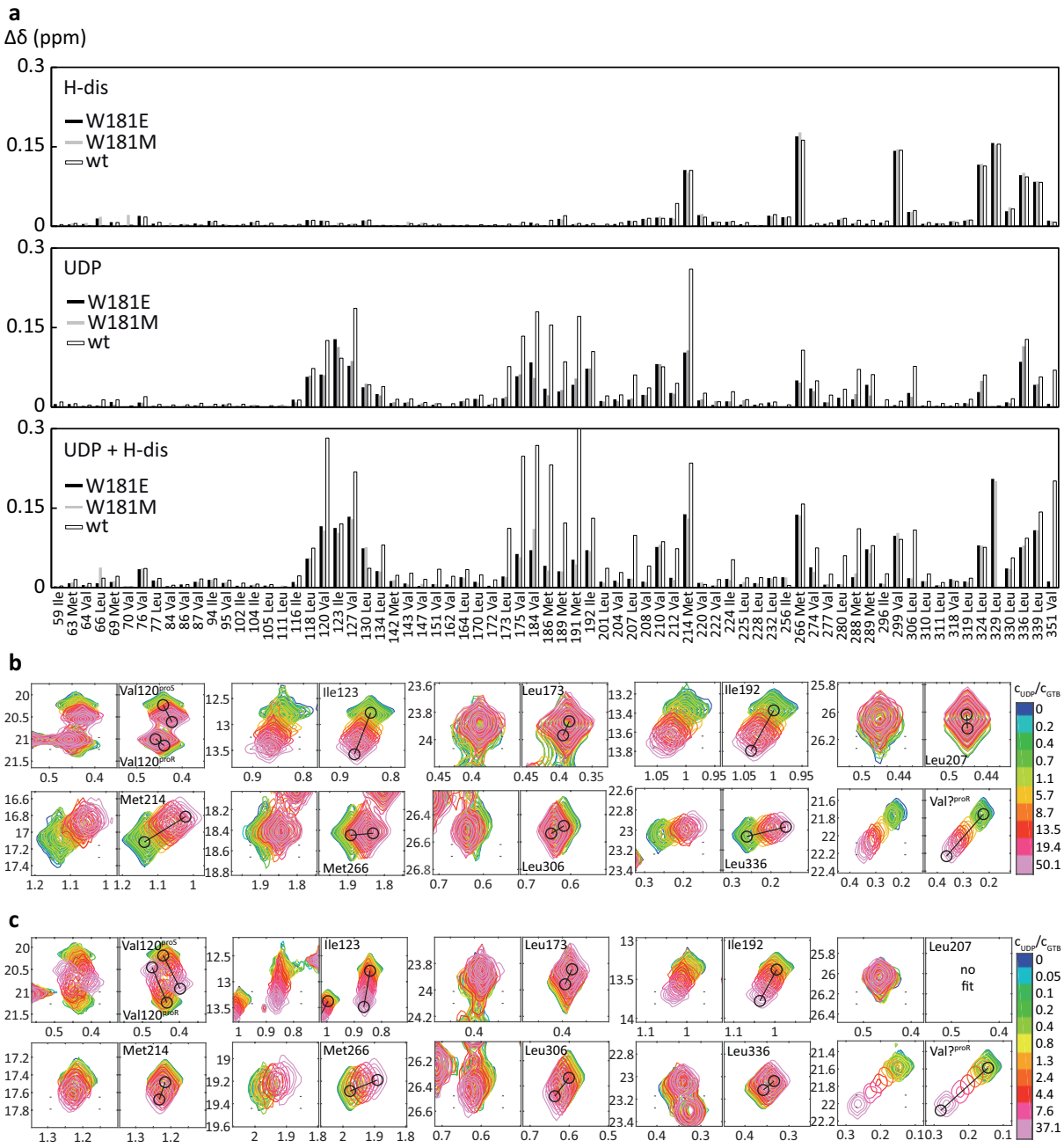

Figure S7 - CSPs for binding of UDP and H-Dis to GTB mutants. Comparison of ligand binding-induced CSPs in wildtype GTB (open bars), GTB Trp181Glu (black bars) and GTB Trp181Met (grey bars) mutants. **a)** Weighted Euclidean distances (Δδ) between peak positions in methyl TROSY spectra of the apo-states and the respective ligand-saturated states (H-disaccharide: top; UDP: center; UDP + H-disaccharide: bottom). **b)** Experimental (left panels) and fitted (right panels) line shapes of selected residues of apo-GTB Trp181Glu titrated with UDP. Relative UDP concentrations are color coded. **c)** as in b) but titration of UDP into GTB Trp181Glu presaturated with H-disaccharide. Compare to Fig. 1 c and d of the main text. Concentrations were: 100 µM GTB Trp181Glu, 200 µM GTB Trp181Met, 280 µM GTB.

Comparison of binding of UDP and H-disaccharide to GTB and two mutants of GTB. CSPs due to binding of H-disaccharide to the GTB-mutants match CSPs observed for wildtype GTB extremely well, indicating similar binding modes (Fig. S7a, first panel). Affinities are slightly different, with the Trp181Glu mutant having an about fivefold better affinity for H-disaccharide and the Trp181Met mutant displaying an almost unchanged K_D value (Table S2). In all cases, binding is characterized by high k_{on} and k_{off} values, reflecting fast exchange (Table S2). CSPs observed upon addition of UDP at saturating concentrations are similar for the mutants but are significantly weaker than CSPs for wildtype GTB (Fig. S7a, second panel). In the presence of saturating concentrations of UDP and H-disaccharide the difference between CSPs for wildtype GTB and for the two mutants is even more

pronounced (Fig. S7a, third panel). Methyl TROSY titrations (Fig. S7b and S7c) do not indicate a change of the time scale of exchange when comparing the titration of UDP to GTB-Trp181Glu mutant to the titration of UDP to GTB-Trp181Glu presaturated with H-disaccharide contrary to what has been observed for wildtype GTB (compare to Fig. 1b and 1c of the main text). Quantitative data evaluation using TITAN analysis reveals two important details. The off-rate constants k_{off} for UDP for both mutants are much higher than for wildtype GTB, and in the presence of H-disaccharide these values decrease only by a factor of about two compared to a one-order of magnitude decrease for wildtype GTB (Table 4). To summarize, the presence of saturating amounts of H-disaccharide has a measurable improvement of the affinities of GTB for UDP, but the large changes in k_{on} and k_{off} values observed for the wildtype enzyme are absent.

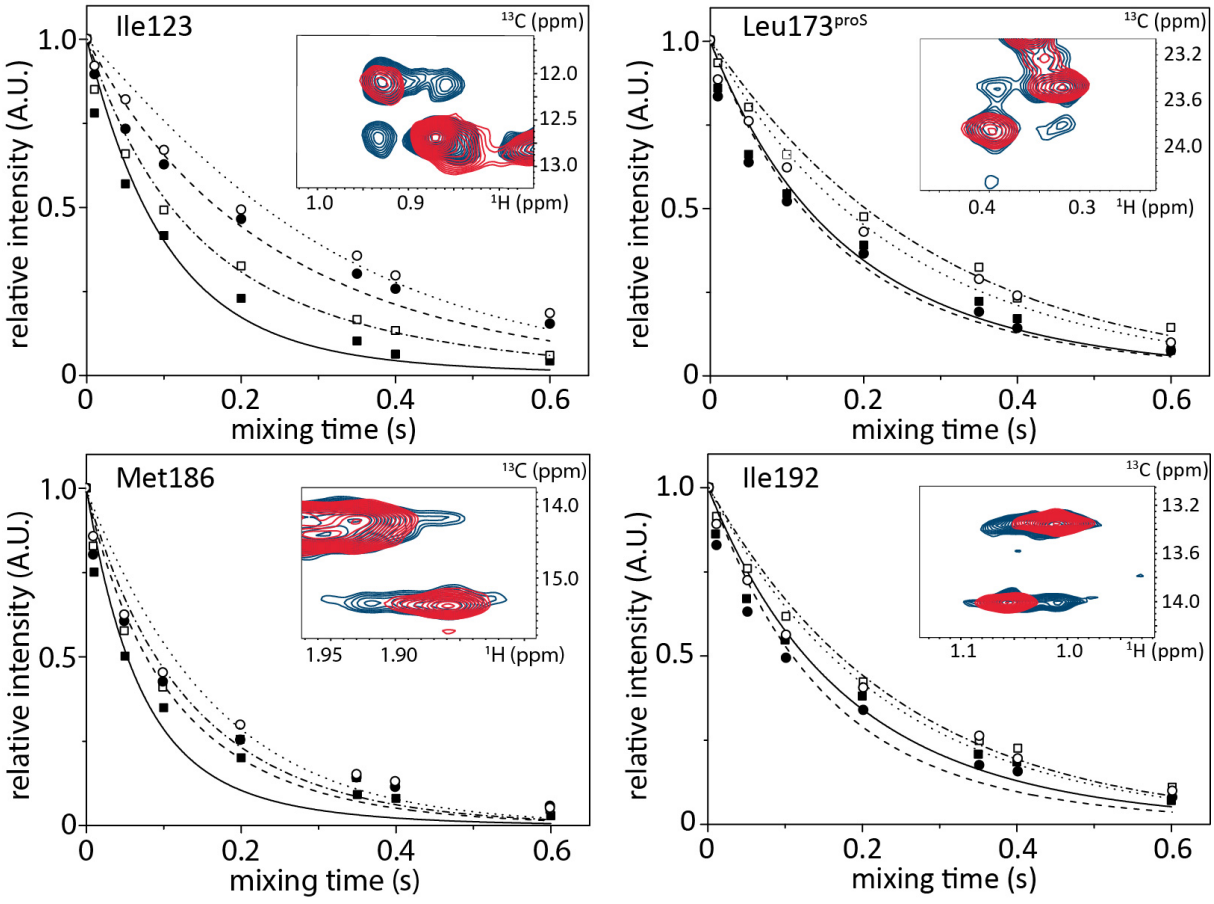

Figure S8 - *ZZ*-exchange data for GTB saturated with H-Dis at half-saturation of UDP. Normalized peak intensities of the direct correlation signals corresponding to Ile^{123}, Leu^{173} (proS), Met^{186} and Ile^{192} methyl groups in the ZZ-exchange experiment of UDP and HDis binding to GTB. The concentrations were 465 µM GTB, 1.5 mM HDis, and 250 µM UDP, leading to saturation with H-Dis and ca. half-saturation with UDP. The intensities are plotted in dependence of the mixing time (··○·· A, --●-- AA, ·-□·- B, −■− BB). A and B correspond to the direct correlation signals in the non-frequency-labeled spectra, and AA and BB to those in the frequency-labeled spectra. Equations describing the time dependency of the direct correlation peaks in a two-site exchanging system are globally and simultaneously fitted to the intensities of the four residues with shared exchange rates[2]. The inserts show zooms of the respective methyl group region in 2D [^{13}C,^{1}H] correlation spectra with (blue) and without (red) frequency-labeling during t_1 at 200 ms mixing time.

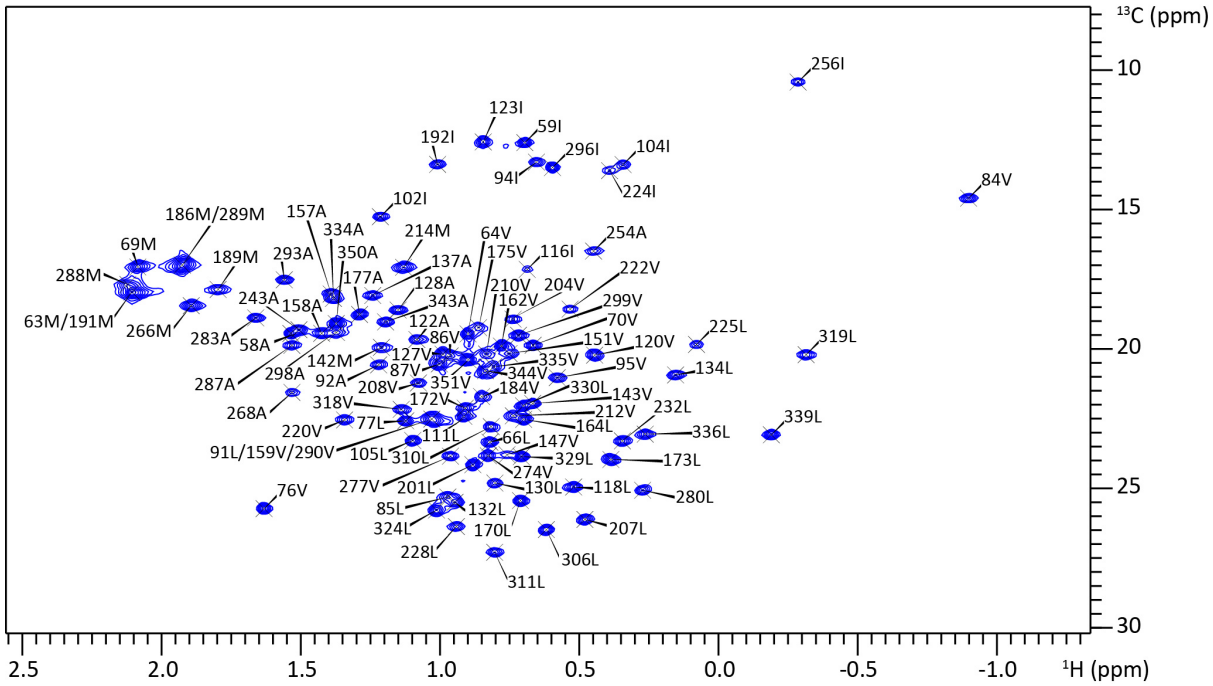

Figure S9 - Assignment of methyl groups for AIL^{proS}MV^{proS} labeled GTB. Sequence-specific resonance assignments of all AIL^{proS}MV^{proS} methyl groups in GTB[3]. 2D methyl-TROSY spectrum of AIL^{proS}MV^{proS} labeled GTB recorded in D_2O phosphate buffer pH* 6.8 at 298 K and 500 MHz ^{1}H frequency. DSS-d_6 served as reference.

Tables

Table S1 - Dissociation- and rate constants for donor-type ligands binding to AAGlyB. Dissociation constants K_D, on- and off-rate constants k_{on} and k_{off} for donor-type ligands binding to AAGlyB from fitting a two-state binding model to methyl TROSY titration data using the TITAN algorithm. Values in brackets are biased by slow hydrolysis of UDP-Gal during the titration. For UDP-GalNAc binding to AAGlyB no titration data could be obtained due to very fast hydrolysis.

	AAGlyB		
	K_D (μM)	k_{on} ($M^{-1}s^{-1}$)	k_{off} (s^{-1})
UDP	37 ± 1	$1.8x10^5$	6.8 ±0.4
UDP-Gal	(64 ± 1)	($8.3x10^4$)	(5.3 ± 0.2)
UDP-Glc	39 ± 1	$<2.3x10^4$	<1
UDP-GalNAc	-	-	-
UDP-GlcNAc	297 ± 9	$7.5x10^4$	22 ± 1

Table S2 - Dissociation- and rate constants for donor-type ligands binding to two GTB mutants. Dissociation constants K_D and on- and off-rate constants (k_{on} , k_{off}) for UDP and H-disaccharide binding to wildtype GTB compared to the mutants GTB Trp181Glu and GTB Trp181Met. Data result from fitting a two-state binding model to methyl TROSY titration data using the TITAN algorithm.

	GTB			GTB Trp181Glu			GTB Trp181Met		
	K_D (μM)	k_{on} ($M^{-1}s^{-1}$)	k_{off} (s^{-1})	K_D (μM)	k_{on} ($M^{-1}s^{-1}$)	k_{off} (s^{-1})	K_D (μM)	k_{on} ($M^{-1}s^{-1}$)	k_{off} (s^{-1})
UDP	161 ± 3	$1.5·10^6$	243 ± 7	738 ± 6	$2.3·10^6$	1700 ± 70	890 ± 10	$1.2·10^6$	1050 ± 60
UDP (H-dis)	103 ± 2	$2.5·10^4$	2.6 ± 0.3	499 ± 4	$1.3·10^6$	650 ± 10	486 ± 7	$1.1·10^6$	560 ± 10
H-dis	164 ± 4	$1.9·10^7$	3100 ± 280	35 ± 1	$3.7·10^7$	1290 ± 30	216 ± 4	$7.0·10^6$	1520 ± 60

Table S3 - Rate constants for UDP binding to GTB:H-Dis from *ZZ*-exchange. Rate constants determined in the ZZ-exchange experiment. Shown are the longitudinal relaxation rates of the indicated methyl groups in the binary (GTB:H-Dis **A**) and ternary binding complex (GTB:H-Dis:UDP **B**), as well as the shared exchange rates between the states.

		Ile^{123}	Leu^{173}	Met^{186}	Ile^{192}
R_1 (s^{-1})	A	2.4 ± 0.4	4.2 ± 0.4	6.3 ± 0.6	4.6 ± 0.5
	B	5.0 ± 0.7	3.3 ± 0.4	8.6 ± 0.9	3.8 ± 0.4
k_{AB} (s^{-1})			**2.0 ± 0.5**		
k_{BA} (s^{-1})			**2.5 ± 0.6**		

References

[1] C. Breton, S. Fournel-Gigleux, M. M. Palcic, *Curr Opin Struct Biol* **2012**, *22*, 540-549.

[2] K. Kloiber, R. Spitzer, S. Grutsch, C. Kreutz, M. Tollinger, *J Biomol NMR* **2011**, *51*, 123-129.

[3] F. Flügge, T. Peters, *J Biomol NMR* **2018**, *70*, 245-259.